CHALMERS
UNIVERSITY OF TECHNOLOGY

Improved Digital Predistortion for Concurrent Multiband Transmission Using Frequency Relocation

Downloaded from: https://research.chalmers.se, 2025-12-04 23:29 UTC

Citation for the original published paper (version of record):
Langborn, B., Fager, C., Hou, R. et al (2023). Improved Digital Predistortion for Concurrent Multiband Transmission Using Frequency Relocation. IEEE MICROWAVE AND WIRELESS TECHNOLOGY LETTERS, 33(7): 1071-1074. http://dx.doi.org/10.1109/LMWT.2023.3257324

N.B. When citing this work, cite the original published paper.

© 2023 IEEE. Personal use of this material is permitted. Permission from IEEE must be obtained for all other uses, in any current or future media, including reprinting/republishing this material for advertising or promotional purposes, or reuse of any copyrighted component of this work in other works.

(article starts on next page)

Improved digital pre-distortion for concurrent multi-band transmission using frequency relocation

Björn Langborn, Christian Fager, Rui Hou, Thomas Eriksson

***Abstract*—In concurrent multi-band settings with large carrier spacings between bands, digital pre-distorter (DPD) implementations face the issue of how to linearize a sparse signal spectrum spanned over large bandwidths at low computational complexity. Frequency relocation is one possible approach, which involves relocating baseband carriers to have reduced frequency spacing with the help of band-limiting functions, to yield a denser and smaller signal bandwidth for the DPD to linearize. In this paper, frequency relocation for transmitters with frequency varying gain and phase is explicitly considered. It is shown that band-wise pre-equalization during frequency relocation can reduce the computational complexity for a certain allowed in-band error.**

***Index Terms*—Digital pre-distortion, DPD, concurrent multi-band, power amplifier, PA, complexity, frequency relocation**

I. Introduction

Modern cellular networks employ multiple frequency bands simultaneously. The low-frequency bands have favorable propagation and penetration properties for network coverage, whereas the high-frequency bands have more abundant spectrum for network capacity. Although concurrent multi-band capability is highly desirable for wireless base-station transmitters, this capability is rarely seen in practical systems due to significant technical challenge in transmitter linearization.

Digital pre-distortion (DPD) techniques are ubiquitous, and well-performing, for linearization and compensation of non-linear distortion in radio frequency power amplifiers (PAs). DPDs enable PAs to operate with high output power and efficiency, whilst still meeting stringent linearity requirements. In contrast to wideband DPDs, which focus on linearizing a wide and contiguous spectrum, a key challenge for multi-band DPD is how to handle sparse, yet wide, bandwidths without drastically increasing DPD complexity. Another challenge is how to address intra-band, and unfilterable inter-band, inter-modulation (IM) that do not arise in single-band transmitters.

DPD for single-band transmitters is a well researched topic, and it serves as a foundation for multi-band DPD. However, single-band DPD solutions are neither computationally efficient for sparse multi-band signals, nor do they explicitly consider the aforementioned types of IM products. When it comes to DPDs specifically for the multi-band setting, solutions like the 2D-DPD and 3D-DPD have been proposed [1]–[4]. The 2D-DPD solutions consider a dual-band input and solve the issue of having sparse, yet wide, bandwidth to linearize by using a DPD per band, so that each DPD can operate at a low complexity. Intermodulation is considered by having the baseband data of each band as input to each DPD. Whilst this works well for the dual-band and tri-band cases, multi-band linearization using such an approach becomes increasingly complex in terms of e.g. the number of basis functions and number of DPDs as the number of bands increase.

A more recent paper presented the concept of frequency relocation for concurrent multi-band linearization [5]. The main idea of frequency relocation is to relocate bands that are widely spread apart to lie closer to one another, since this allows the DPD to operate on data sampled at a lower rate, which reduces computational complexity. However, considering that the gain and phase response of a transmitter can vary significantly over large frequency ranges, the frequency relocated system response will exhibit the same variations but over a smaller bandwidth. This poses a challenging compensation problem for the DPD. This paper seeks to address how transmitter gain and phase variations can be taken into consideration, by introducing band-wise pre-equalization blocks in the schematic.

In the paper that follows, Section II describes frequency relocation in more detail. In Section III, the proposed frequency relocation scheme using pre-equalization coefficients is presented. Lastly, Section IV elaborates on the experimental setup and results to verify the proposed approach.

II. Frequency relocation system description

A schematic outlining the steps involved in frequency relocation can be seen in Fig. 1. Starting from the right side, the goal is to produce an output y as similar as possible to y_d, the desired output. Given that the PA has some gain variation over frequency, indicated in solid lines in the graph above the PA, and some non-linearity, then a specific u must be input to achieve y at the output. It is seen from the schematic that this u is produced by relocating the bands in u'. Furthermore, u' is obtained by a non-linear mapping from y'_d using the DPD, and y'_d obtained by relocating the input signal y_d.

The issue with wide, yet sparse, bandwidth is here solved by relocating all bands to a lower frequency range during linearization. Additionally, IM products are accounted for by the choice of frequency spacing, as detailed in [5]. Briefly stated, if the original frequency spacing is even then the relocated frequencies are chosen to be evenly spaced as well, so that all IM end up band-centered. A bandwidth large enough for characterizing the PA's response around each band is chosen, which has been done in previous works as well as only frequency components around each carrier are typically significant for the PA output formulation [6], [7]. The separation of relocated bands is kept to have non-overlapping spectral regrowth. If the original frequency spacing is uneven,

Manuscript received December 20, 2022; Revised Febuary 9, 2023. This work was supported by Vinnova, the Swedish Energy Agency and Formas via the strategic innovation programme Smarter Electronic Systems. Björn Langborn and Thomas Eriksson are with the Department of Electrical Engineering, Chalmers University of Technology, 412 96, Gothenburg, Sweden (e-mail: langborn@chalmers.se; thomase@chalmers.se). Christian Fager is with the Department of Microtechnology and Nanoscience, Chalmers University of Technology, 412 96 Gothenburg, Sweden (e-mail: christian.fager@chalmers.se). Rui Hou is with Ericsson AB, 164 40 Stockholm, Sweden (e-mail: rui.hou@ericsson.com).

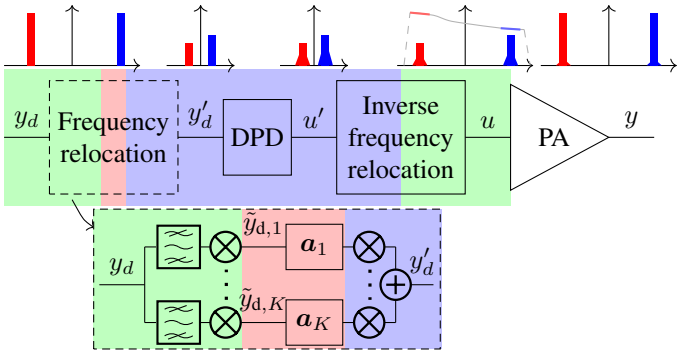

Fig. 1. Simplified schematic of the frequency relocation concept, with the proposed modification elaborated below. The lines in the u spectrum indicate the gain profile of the PA. The colored regions refer to the sample rates of signals in that region. Here, red, blue and green corresponds to low, medium and high sample rates respectively. The symbols $\boldsymbol{a}_1, ...\boldsymbol{a}_K$ are vectors, and refer to FIR filter coefficients for pre-equalization.

IM will end up out-of-band and one typically places bands as close as possible without getting IM partially in-band.

III. Proposed DPD schematic

A key observation to note from Fig. 1 is the fact that the PA's complex gain can vary across different frequencies. These variations typically vary smoothly over a continuous range of frequencies, and within each band the variations are likely not very large. However, for large carrier spacings these variations can yield significantly different gain and phase responses for the different bands in a multi-band signal. These observations are exemplified in Figure 2b, and it can be understood that the optimal input u to the PA will reflect these gain variations. Furthermore, when inversely relocating the signal u to u' it is clear that the gain transition between bands in u' becomes more abrupt. So if the bands in y'_d are unaltered from their magnitudes and phases in y_d, the DPD has to compensate for the gain transition, in addition to the effects that occur with a more frequency flat response of the PA. From the time-frequency duality it can be realised that if the DPD has to compensate a sharp transition in the frequency domain, this corresponds to that the DPD requires a longer memory in time. Thus, the DPD complexity increases. In [5], no explicit consideration to this observation is made.

However, it was noted that the variations within each band are not expected to be very large. So if the abrupt changes in gain and phase between bands are handled band-wise, i.e. in a small frequency region around each carrier instead of over the whole frequency span, we expect that it can be done at a very low complexity per band. Thus, the novelty of this work is to address the sharp transitions by using band-wise pre-equalization filters to get y'_d, to make the DPD mapping from y'_d to u' easier. As detailed in the experimental results, this can both improve performance and reduce complexity compared to the original frequency relocation technique.

The proposed schematic is presented in Fig. 1. Compared to [5], FIR filters $\boldsymbol{a}_1, ...\boldsymbol{a}_K$ for each band are introduced here, that can adjust adjust the signal magnitudes and phases in y'_d. Worth noting is that if the PA gain and phase is equal in each band then the optimal choice of coefficients are $\boldsymbol{a}_i = 1$, $i = 1, .., K$ and the proposed method becomes equivalent to [5].

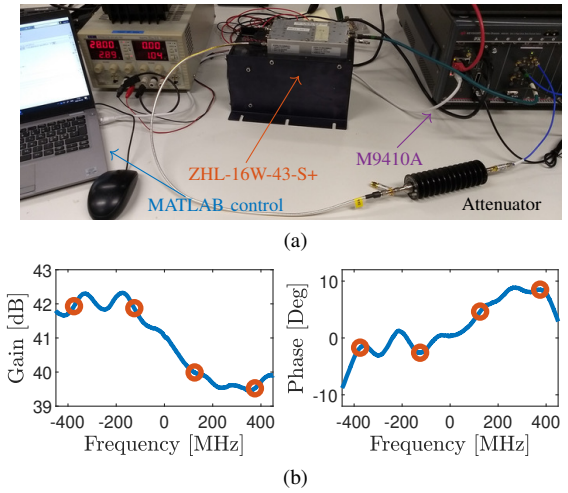

Fig. 2. Experimental setup for the DPD measurements in 2a, and PA gain characterization in 2b. For 2b, the linear gain and phase (magnitude and phase of S_{21}) of the PA at center carrier 3.35 GHz, is viewed in the baseband domain. The dots highlight the band placement for the results in Table I.

Determining the coefficients in $\boldsymbol{a}_1, ..., \boldsymbol{a}_K$ requires joint optimization with the DPD coefficients. The normalized mean square error (NMSE) $\epsilon_{y_d} = \Sigma_i(y_d[i] - y[i])^2/\Sigma_i y_d^2[i]$ is chosen as the performance metric to be minimized, and the minimization is done iteratively. First, an initial choice of $\boldsymbol{a}_1, ..., \boldsymbol{a}_K$ can be made e.g. based on the linear gain characteristics of the PA. Secondly, linear least squares optimization is performed for the DPD to minimize $\Sigma_i(y'_d[i] - u'[i])^2/\Sigma_i y'^2_d[i]$. Then, ϵ_{y_d} can be computed after measuring y. After this, $\boldsymbol{a}_1, ..., \boldsymbol{a}_K$ are updated using numerical optimization [8], and the iteration starts over. The goal is to find the best $\boldsymbol{a}_1, ..., \boldsymbol{a}_K$ to simplify the DPD mapping from y'_d to u', resulting in a lower ϵ_{y_d} for a given DPD complexity.

Whilst the proposed scheme is a special case of a general cascade DPD structure, previous work such as [9]–[12] are not ideally suited to, with low complexity, address the aggravation of memory effects and gain transitions caused by frequency relocation. Thereby, this work is of use to reduce complexity for frequency relocation DPDs with sparse multi-band signals.

IV. Experimental setup and results

To demonstrate the proposed schematic, a Keysight M9410A VXT PXI Vector Transceiver has been used to transmit signals through a MiniCircuits ZHL-16W-43-S+ power amplifier, as seen in Figure 2a. The Peak-to-Average Power Ratio of y_d was reduced to 9 dB using iterative clipping-and-filtering. Iterative Learning Control [13] was adopted for finding an optimal input signal u to linearize the PA, after which Generalized Memory Polynomial (GMP) [6] models of varying orders were adapted to map y'_d to u'. The GMP models are characterized by their non-linearity order P, memory depth M and cross-memory depth G. Using all non-linearity terms, the coefficient complexity of the DPD can be calculated as

$$C_{\text{DPD}} = P(M+1)(2G+1)\,, \tag{1}$$

whilst the total coefficient complexity becomes

$$C_{\text{tot}} = P(M+1)(2G+1) + KM_{\text{p}}\,, \tag{2}$$

TABLE I

ACLR AND NMSE FROM QUAD-BAND MEASUREMENT WITH NO DPD, FREQUENCY RELOCATION WITHOUT OR WITH A PRE-EQUALIZATION COEFFICIENT PER BAND, OR WITHOUT FREQUENCY RELOCATION, FOR DIFFERENT GMP ORDERS. SCALAR, BAND-WISE, POST-EQUALIZATION IS USED FOR EACH MEASUREMENT. FOR COMPACTNESS, EACH ACLR VALUE CORRESPONDS TO THE SIDE OF THE BAND WITH MOST POWER LEAKAGE.

ACLR [dBc] **NMSE** [dB]	No DPD				DPD w/o frequency relocation				Yu et al.[5]				This work			
	2.98 GHz	3.23 GHz	3.48 GHz	3.73 GHz	2.98 GHz	3.23 GHz	3.48 GHz	3.73 GHz	2.98 GHz	3.23 GHz	3.48 GHz	3.73 GHz	2.98 GHz	3.23 GHz	3.48 GHz	3.73 GHz
P=7,M=3,G=0	-39.1	-38.7	-36.9	-37.6	-49.1	-48.9	-49.0	-48.5	-47.8	-48.1	-46.4	-48.7	-48.6	-47.2	-47.3	-48.4
	-31.2	**-30.7**	**-29.1**	**-29.8**	**-41.9**	**-41.6**	**-42.3**	**-41.5**	**-38.2**	**-40.1**	**-37.4**	**-36.6**	**-39.5**	**-39.0**	**-39.2**	**-39.2**
P=7,M=3,G=1					-50.5	-49.3	-49.6	-49.9	-48.9	-49.0	-49.6	-49.3	-49.1	-49.4	-48.6	-49.4
					-43.7	**-42.0**	**-43.0**	**-43.1**	**-36.1**	**-39.3**	**-37.9**	**-41.1**	**-41.6**	**-40.7**	**-40.6**	**-41.9**
P=7,M=5,G=1					-50.6	-49.3	-49.7	-49.9	-50.4	-49.5	-50.2	-49.9	-49.9	-49.3	-48.8	-49.9
					-43.7	**-42.1**	**-42.9**	**-43.2**	**-42.6**	**-39.9**	**-37.9**	**-42.6**	**-42.1**	**-41.5**	**40.8**	**-42.2**

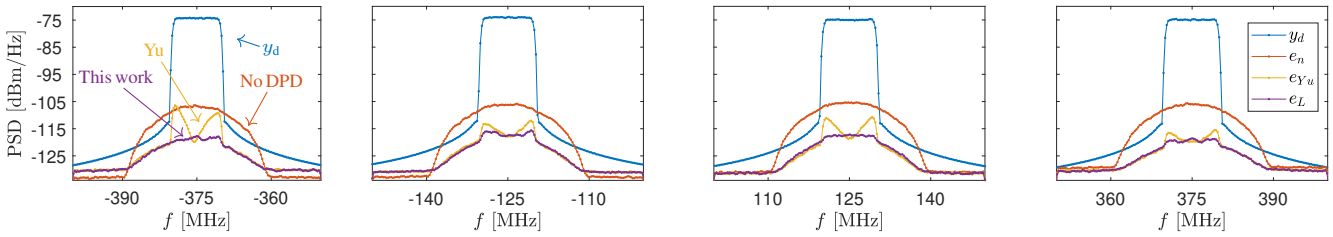

Fig. 3. Power spectral density (PSD) of the desired quad-band signal y_d (in blue), and the errors $e_{\text{Yu}} = y_{\text{Yu}} - y_d$, $e_{\text{L}} = y_{\text{L}} - y_d$, $e_n = y_n - y_d$ in each band, seen in yellow (Yu et. al method [5]), purple (this work) and red (no DPD) respectively. The GMP order is $P = 7$, $M = 3$, $G = 1$.

where M_{p} is the pre-equalization filter length in each of the K bands. For the following results, $M_{\text{p}} = 1$ was used.

A complex baseband signal y_d, containing four frequency spaced 10 MHz-bands centered around -375, -125, 125 and 375 MHz was sent from Matlab to the M9410A, upconverted with a carrier of 3.35 GHz and transmitted. Relocated frequencies were chosen as -75, -25, 25 and 75 MHz. The low, medium and high sampling rates (corresponding to red, blue and green regions in Figure 1) were chosen as 50 MHz, 200 MHz and 1200 MHz.

In Figure 3, a desired quad-band output signal (in blue) and the errors $e = y - y_d$ for the cases of no DPD (in red), Yu et. al.'s method [5] (in yellow) and the proposed method (in purple) are shown. The corresponding NMSE, and largest adjacent channel leakage ratio (ACLR) for each band, are found in Table I. Firstly, it is seen that the addition of a pre-equalization coefficient per band improves linearization performance when the GMP complexity remains the same, comparing this work to [5]. Secondly, it can be seen that not even for a GMP of order P=7, M=5, G=1 can the method of [5] reach an NMSE below -39 dB for all bands, whilst this is achieved already at P=7, M=3, G=0 for this work. Using (1), the case P=7, M=5, G=1 results in 126 DPD coefficients. For the proposed method, using (2) the case P=7, M=3, G=0 results in a total of 32 coefficients. Thirdly, it is seen that linearization without frequency relocation performs best, though it requires 6 times higher sample rate for the DPD data, which may be practically unfeasible.

Finally, the results of a dual-band measurement varying M_p can be seen in Table II. Here, the bandwidth of each signal is 50 MHz and the bands are centered around -220 and 220 MHz respectively, with a carrier frequency of 3.35 GHz. Relocated frequencies were -125 and 125 MHz, and the sample rates chosen as 250, 520 and 720 MHz respectively. Relocated frequencies were -125 and 125 MHz, and the low, medium and high sample rates chosen as 250, 520 and 720 MHz respectively.

TABLE II

ACLR AND NMSE FROM DUAL-BAND MEASUREMENT USING NO DPD, AND FREQUENCY RELOCATION WITHOUT OR WITH PRE-EQUALIZATION WITH M_p COEFFICIENTS PER BAND. THE GMP MEMORY M VARIES, BUT WITH FIXED $P = 7$, $G = 0$. SCALAR, BAND-WISE, POST-EQUALIZATION IS USED FOR EACH MEASUREMENT. FOR COMPACTNESS, EACH ACLR VALUE CORRESPONDS TO THE SIDE OF THE BAND WITH MOST POWER LEAKAGE.

ACLR [dBc] **NMSE** [dB]	No DPD	Yu et al. [5]			This work		
		M=2	M=3	M=6	M=2, M_p=1	M=2, M_p=3	M=3, M_p=3
3.13 GHz	-36.2	-45.8	-46.3	-46.4	-46.8	-46.8	-47.7
	-27.9	**-30.4**	**-38.0**	**-39.4**	**-37.2**	**-41.1**	**-42.2**
3.57 GHz	-34.8	-45.7	-46.4	-46.5	-44.7	-44.8	-45.9
	-27.3	**-34.4**	**-40.5**	**-40.6**	**-37.7**	**-38.0**	**-39.3**

respectively.

Firstly, it can be seen from Table II that in terms of NMSE, increasing M_p can move some of complexity from the DPD to the FIR-filters, comparing especially the case Yu et al. $M = 3$ against the case $M = 2$, $M_p = 3$ for the proposed approach. That can be advantageous, since the FIR-filter computations are performed at a lower sample rate and requires no additional cost for generating basis functions [14]. Secondly, it can be seen that cases occur where it is more computationally efficient to increase the FIR-depth than to increase the DPD memory. Looking at the case $M = 3, M_p = 3$, it corresponds to a coefficient complexity of 34 according to (2). In comparison, $M = 6$ corresponds to a complexity of 49 according to (1).

V. CONCLUSION

Using band-wise pre-equalization in a frequency relocating DPD linearization scheme, the concurrent multi-band linearization performance can be improved at a lower coefficient complexity. The method improves upon previous work [5] when the PA gain and phase vary for different carriers.

REFERENCES

[1] Y. J. Liu, W. Chen, J. Zhou, B. H. Zhou, and F. M. Ghannouchi, "Digital predistortion for concurrent dual-band transmitters using 2-D modified memory polynomials," *IEEE Transactions on Microwave Theory and Techniques*, vol. 61, no. 1, pp. 281–290, 2013, ISSN: 00189480. DOI: 10.1109/TMTT.2012.2228216.

[2] S. A. Bassam, M. H. Helaoui, and F. M. Ghannouchi, "2-D digital predistortion (2-D-DPD) architecture for concurrent dual-band transmitters," *IEEE Transactions on Microwave Theory and Techniques*, vol. 59, no. 10 PART 1, pp. 2547–2553, 2011, ISSN: 00189480. DOI: 10.1109/TMTT.2011.2163802.

[3] M. Younes, A. Kwan, M. Rawat, and F. M. Ghannouchi, "Three-dimensional digital predistorter for concurrent tri-band power amplifier linearization," *IEEE MTT-S International Microwave Symposium Digest*, vol. 1, no. 2, pp. 1–4, 2013, ISSN: 0149645X. DOI: 10.1109/MWSYM.2013.6697635.

[4] E. Zenteno and D. Ronnow, "MIMO Subband Volterra Digital Predistortion for Concurrent Aggregated Carrier Communications," *IEEE Transactions on Microwave Theory and Techniques*, vol. 65, no. 3, pp. 967–979, 2017, ISSN: 00189480. DOI: 10.1109/TMTT.2016.2630066.

[5] C. Yu, J. Xia, X. W. Zhu, and A. Zhu, "Single-Model Single-Feedback Digital Predistortion for Concurrent Multi-Band Wireless Transmitters," *IEEE Transactions on Microwave Theory and Techniques*, vol. 63, no. 7, pp. 2211–2224, 2015, ISSN: 00189480. DOI: 10.1109/TMTT.2015.2429633.

[6] D. R. Morgan, Z. Ma, J. Kim, M. G. Zierdt, and J. Pastalan, "A generalized memory polynomial model for digital predistortion of RF power amplifiers," *IEEE Transactions on Signal Processing*, vol. 54, no. 10, pp. 3852–3860, 2006, ISSN: 1053587X. DOI: 10.1109/TSP.2006.879264.

[7] F. Mkadem, A. Islam, S. Boumaiza, and S. Member, "Multi-Band Complexity-Reduced Generalized Memory-Polynomial Power-Amplifier Digital Predistortion," *IEEE Transactions on Microwave Theory and Techniques*, vol. 64, no. 6, pp. 1763–1774, 2016. DOI: 10.1109/TMTT.2016.2561279.

[8] J. C. Lagarias, J. A. Reeds, M. H. Wright, and P. E. Wright, "Convergence Properties of the Nelder-Mead Simplex Method in Low Dimensions," *SIAM Journal on Optimization*, vol. 9, no. 1, pp. 112–147, 1998. DOI: 10.1137/S1052623495297820.

[9] S. Wang, M. Abi Hussein, O. Venard, and G. Baudoin, "Optimal Sizing of Two-Stage Cascaded Sparse Memory Polynomial Model for High Power Amplifiers Linearization," *IEEE Transactions on Microwave Theory and Techniques*, vol. 66, no. 9, pp. 3958–3965, 2018, ISSN: 00189480. DOI: 10.1109/TMTT.2018.2838126.

[10] M. Rawat, F. M. Ghannouchi, and K. Rawat, "Three-layered biased memory polynomial for dynamic modeling and predistortion of transmitters with memory," *IEEE Transactions on Circuits and Systems I: Regular Papers*, vol. 60, no. 3, pp. 768–777, 2013, ISSN: 15498328. DOI: 10.1109/TCSI.2012.2215740.

[11] F. M. Barradas, L. C. Nunes, J. C. Pedro, T. R. Cunha, P. M. Lavrador, and P. M. Cabral, "Accurate Linearization with Low-Complexity Models Using Cascaded Digital Predistortion Systems," *IEEE Microwave Magazine*, vol. 16, no. 1, pp. 94–103, 2015. DOI: 10.1109/MMM.2014.2367864.

[12] H. Ku, M. D. McKinley, and J. S. Kenney, "Extraction of accurate behavioral models for power amplifiers with memory effects using two-tone measurements," *IEEE MTT-S International Microwave Symposium Digest*, vol. 1, pp. 139–142, 2002, ISSN: 0149645X. DOI: 10.1109/MWSYM.2002.1011578.

[13] J. Chani-Cahuana, P. N. Landin, C. Fager, and T. Eriksson, "Iterative Learning Control for RF Power Amplifier Linearization," *IEEE Transactions on Microwave Theory and Techniques*, vol. 64, no. 9, pp. 2778–2789, 2016, ISSN: 00189480. DOI: 10.1109/TMTT.2016.2588483.

[14] A. S. Tehrani, H. Cao, S. Afsardoost, T. Eriksson, M. Isaksson, and C. Fager, "A Comparative analysis of the complexity/accuracy tradeoff in power amplifier behavioral models," *IEEE Transactions on Microwave Theory and Techniques*, vol. 58, no. 6, pp. 1510–1520, Jun. 2010, ISSN: 00189480. DOI: 10.1109/TMTT.2010.2047920.